Journal of Molecular Structure (Theochem), 234 (1991) 95–126
Elsevier Science Publishers B.V., Amsterdam

Determination and use of response densities

Elfi Kraka, Jürgen Gauss[1] and Dieter Cremer[2]

Theoretical Chemistry, University of Göteborg, Kemigården 3, S-41296 Göteborg (Sweden)

(Received 2 September 1990)

Abstract

One-electron properties of molecules can be calculated either as an expectation value of the corresponding one-electron operator or as the response of the molecule with regard to a perturbation that leads to the property in question. Advantages of the later approach are discussed and general ways to calculate response properties for Møller–Plesset perturbation (MPn) and quadratic CI (QCI) methods are given. Response properties (electron density distribution, atomic charges, dipole moments, quadrupole moments) of 20 small molecules have been calculated by nine different methods using the 6-31G(d,p) and 6-311G(2d,2p) (or MC-311G(2d,2p) for second row atoms) basis set. For some test cases, it is shown that correlation corrections to response properties oscillate depending on the method and basis set. MPn values of the response properties have not converged for $n=4$ and probably also not for $n=5$ or 6. This is concluded from an analysis of QCI results in terms of MP perturbation theory.

INTRODUCTION

Quantum mechanically, a one-electron property is defined as the expectation value of the corresponding one-electron operator $\hat{O}$

$$\langle \hat{O} \rangle = \langle \Phi | \hat{O} | \Phi \rangle \tag{1}$$

However, this approach leads to ambiguities for those ab initio methods for which a well-defined wave function does not exist. Many electron correlation methods such as the various Møller–Plesset (MP) perturbation approaches (MP2, MP3, MP4) [1–5], CI with size-consistency corrections [6], CEPA [7], CPF [8], and the recently developed QCI methods [9,10] belong to this class. In these cases, it is appropriate to calculate a one-electron property by determining the response of a molecular state $|\Phi_0\rangle$ under the impact of a perturbation λ that is responsible for the molecular property [11–13]. The molecular energy E in the presence of a perturbation is determined as the ex-

[1]Present address: Quantum Theory Project, Departments of Chemistry and Physics, University of Florida, Gainesville, FL 32611, U.S.A.
[2]To whom correspondence should be addressed.

pectation value of the operator $\hat{H}+\lambda\hat{H}_1$ where $\hat{H}$ is the unperturbed Hamiltonian and $\hat{H}_1$ is the perturbation operator corresponding to λ. The energy E becomes a function of the perturbation λ and, therefore, can be expanded for small λ in the power series given by

$$E(\lambda) = \langle \Phi_0 | \hat{H}+\lambda\hat{H}_1 | \Phi_0 \rangle$$
$$= E_0 + \lambda E_1 + (1/2)\lambda^2 E_2 + (1/6)\lambda^3 E_3 + \ldots \quad (2)$$

Applying the Hellmann–Feynman theorem leads to

$$\mathrm{d}E(\lambda)/\mathrm{d}\lambda|_{\lambda=0} = \langle \Phi_0 | \hat{H}_1 | \Phi_0 \rangle$$
$$= E_1 \quad (3)$$

which shows that the one-electron property can be evaluated either as a derivative of E with regard to λ or as an expectation value. However, the equivalence of the two approaches only holds if the Hellmann–Feynman theorem is fulfilled. For many correlation methods, e.g. for CI and coupled cluster (CC) methods, this is not true and therefore the derivative and the expectation value approaches lead to different values of the one-electron property in question. In these cases, it is advantageous to use the derivative approach, which is more closely related to experiment, where properties are determined by measuring the response of a molecule with regard to an external perturbation. Also, the derivative approach preserves the continuity of the potential energy surface $E(\lambda)$ with regard to λ. In the expectation value approach, however, there exists no clear relationship between the energy surface $E(\lambda)$ and the molecular property.

When λ represents a static electric field $\mathscr{F}$, then the perturbed Hamiltonian is given by $\hat{H}+\mathscr{F}\hat{r}$ and the corresponding one-electron property is the molecular dipole moment μ

$$\langle \Phi_0 | \hat{r} | \Phi_0 \rangle = E_1$$
$$= -\mu \quad (4)$$

i.e. μ is the first-order response property of a molecule with regard to an external static electric field. For SCF wave functions, both approaches lead to the same result and therefore μ is normally calculated as the expectation value of $\hat{r}$. For most correlation methods, however, the energy derivative E_1 is not equal to the expectation value of $\hat{r}$ and an evaluation of μ via energy derivatives is preferred.

Other one-electron properties (higher multipole moments such as quadrupole and octopole moments, electric field gradients, magnetic moments, electron densities, spin densities, etc.) can be defined in the same way as μ. For example, the total electron density $\rho(\mathbf{r}_p)$ at a point $\mathbf{r}_p$ is the response of the

molecule to the perturbation λ that corresponds to the one-electron operator $\hat{\delta}(\mathbf{r}_p - \mathbf{r})$, which is the Dirac delta operator. By using the Hellmann–Feynman theorem, one gets

$$dE(\lambda)/d\lambda|_{\lambda=0} = \langle \Phi_0 | \hat{\delta}(\mathbf{r}_p - \mathbf{r}) | \Phi_0 \rangle$$
$$= E_1 = \rho(\mathbf{r}_p) \tag{5}$$

When ρ is expanded in terms of basis functions used to calculate energy and wave function, eqn. (6) is obtained.

$$dE(\lambda)/d\lambda|_{\lambda=0} = \sum_{\mu\nu} \boldsymbol{P}^{\mathrm{Res}}_{\mu\nu} \chi_\mu(\mathbf{r}_p)\chi_\nu(\mathbf{r}_p) \tag{6}$$

where $\boldsymbol{P}^{\mathrm{Res}}_{\mu\nu}$ is the response density matrix [11–13]. In the case of an SCF wave function $\boldsymbol{P}^{\mathrm{Res}}$ is identical with the SCF density matrix. For correlation methods without a well-defined wave function, eqns. (5) and (6) provide, for the first time, a rigorous definition of electron density distribution $\rho(\mathbf{r})$ and density matrix $\boldsymbol{P}$. But even if the density matrix can be calculated via the expectation value approach and is not identical with the response density matrix as, for example, in the case of CI methods, $\boldsymbol{P}^{\mathrm{Res}}$ seems to us the better choice and should therefore be used in general when analyzing correlated wave functions. In addition to correlation effects, the response density also includes those effects that are due to orbital relaxation caused by the perturbation λ. The latter effects are calculated when solving the coupled perturbed Hartree–Fock (CPHF) equations [14].

For correlation methods, $\boldsymbol{P}^{\mathrm{Res}}$ can be expressed as a sum of the SCF density matrix and the correlation corrections $\boldsymbol{P}^{\mathrm{Cor}}$

$$\boldsymbol{P}^{\mathrm{Res}} = \boldsymbol{P}^{\mathrm{SCF}} + \boldsymbol{P}^{\mathrm{Cor}} \tag{7}$$

$\boldsymbol{P}^{\mathrm{Cor}}$ provides a useful tool when analyzing correlation effects in molecules.

With the definition of $\boldsymbol{P}^{\mathrm{Res}}$, any one-electron property can be written as

$$O = dE(\lambda)/d\lambda|_{\lambda=0}$$
$$= \sum_{\mu\nu} \boldsymbol{P}^{\mathrm{Res}}_{\mu\nu} \langle \chi_\mu | \hat{O} | \chi_\nu \rangle \tag{8}$$

thus leading to a computationally straightforward procedure for calculating one-electron properties. For example, the three components of the dipole moment are given as a contraction of the elements of $\boldsymbol{P}^{\mathrm{Res}}$ with the appropriate dipole moment integrals calculated in the space of the basis functions.

$$dE(\mathscr{F})/d\mathscr{F}_\alpha|_{\mathscr{F}_\alpha=0} = -\mu_\alpha$$
$$= \sum_{\mu\nu} \boldsymbol{P}^{\mathrm{Res}}_{\mu\nu} \langle \chi_\mu | \hat{\mathbf{r}}_\alpha | \chi\nu \rangle \quad \text{with } \alpha = x,y,z \tag{9}$$

In geometry optimizations with correlation methods, the response density is needed to evaluate the forces on the nuclei. Hence, $\boldsymbol{P}^{\mathrm{Res}}$ is routinely obtained at no extra cost once the optimized geometry has been determined [11–13,15]. This we will show in the following section where we derive a general expression

for the analytical energy gradient for MP and quadratic CI (QCI) methods [16–18].

ANALYTICAL ENERGY GRADIENTS FOR MP METHODS

The MP2 energy can be written as [2]

$$E(\mathrm{MP2}) = (1/4)\sum_{ij}\sum_{ab} a(ij,ab)\langle ij\|ab\rangle \tag{10}$$

where $a(ij,ab)$ denotes the first-order correction to the HF wave function

$$a(ij,ab) = \frac{\langle ij\|ab\rangle}{\epsilon_i+\epsilon_j-\epsilon_a-\epsilon_b} \tag{11}$$

and the double bar integral is defined as

$$\langle pq\|rs\rangle = \int\int \phi_p^*(1)\phi_q^*(2)\,|\mathbf{r}_1-\mathbf{r}_2|^{-1}[\phi_r(1)\phi_s(2)-\phi_s(1)\phi_r(2)]\,\mathrm{d}\tau_1\mathrm{d}\tau_2 \tag{12}$$

Note that i, j, k, l, etc. refer to occupied, a, b, c, d, etc. to virtual, and p, q, r, s, etc. to general orbitals. The energy gradient is given by [16]

$$\mathrm{d}E(\mathrm{MP2})/\mathrm{d}\lambda = (1/2)\sum_{ij}\sum_{ab} a(ij,ab)\langle ij\|ab\rangle^{\lambda}$$
$$-(1/2)\sum_{ijk}\sum_{ab} a(ij,ab)\epsilon_{ik}^{\lambda} a(kj,ab) + (1/2)\sum_{ij}\sum_{abc} a(ij,ab)\epsilon_{ac}^{\lambda} a(ij,cb) \tag{13}$$

with

$$\langle ij\|ab\rangle^{\lambda} = \sum_{\mu\nu\sigma\rho} c_{\mu i}c_{\nu j}c_{\sigma a}c_{\rho b}\,\partial\langle\mu\nu\|\sigma\rho\rangle/\partial\lambda + \sum_c [U_{ci}^{\lambda}\langle cj\|ab\rangle + U_{cj}^{\lambda}\langle ic\|ab\rangle]$$
$$+\sum_k [U_{ka}^{\lambda}\langle ij\|kb\rangle + U_{kb}^{\lambda}\langle ij\|ak\rangle] - (1/2)\sum_k [S_{ki}^{\lambda}\langle kj\|ab\rangle + S_{kj}^{\lambda}\langle ik\|ab\rangle]$$
$$-(1/2)\sum_c [S_{ca}^{\lambda}\langle ij\|cb\rangle + S_{cb}^{\lambda}\langle ij\|ac\rangle] \tag{14}$$

In eqn. (13), the U_{qp}^{λ} are used to expand $\partial c_{\mu p}/\partial\lambda$ in terms of the unperturbed coefficients $c_{\mu q}$

$$\frac{\partial c_{\mu p}}{\partial\lambda} = \sum_q U_{qp}^{\lambda} c_{\mu q} \tag{15}$$

The perturbed orbitals are orthonormal and, hence, eqn. (16) holds.

$$U_{pq}^{\lambda} + S_{pq}^{\lambda} + U_{qp}^{\lambda} = 0 \tag{16}$$

with

$$S_{pq}^{\lambda} = \sum_{\mu\nu} c_{\mu p}(\partial S_{\mu\nu}/\partial\lambda)c_{\nu q} \tag{17}$$

In order to avoid problems in case of degeneracies or near degeneracies of orbital energies, it is convienent to set [19]

$$U_{ij}^{\lambda} = -(1/2)S_{ij}^{\lambda} \tag{18}$$

$$U^{\lambda}_{ab} = -(1/2)S^{\lambda}_{ab} \tag{19}$$

The derivatives of the Lagrangian multipliers ϵ_{pq} are given by

$$\epsilon^{\lambda}_{pq} = F^{(\lambda)}_{pq} + \sum_a \sum_i U^{\lambda}_{ai} A_{pqai} - (1/2)\sum_{ij} S^{\lambda}_{ij} A_{pqij} - (1/2) S^{\lambda}_{pq}(\epsilon_p + \epsilon_q) \tag{20}$$

with

$$A_{pqrs} = \langle pr \| qs \rangle + \langle ps \| qr \rangle \tag{21}$$

and

$$F^{(\lambda)}_{pq} = \sum_{\mu\nu} c_{\mu p} F^{(\lambda)}_{\mu\nu} c_{\nu q}$$

$$= \sum_{\mu\nu} c_{\mu p} [\partial h_{\mu\nu}/\partial\lambda + \sum_r \sum_{\sigma\rho} c_{\sigma r} c_{\rho r} \partial \langle \mu\sigma \| \nu\rho \rangle / \partial\lambda] c_{\nu q} \tag{22}$$

Introducing [17,18]

$$T^{(2)}_{\mu\nu\sigma\rho} = (1/2)\sum_{ij}\sum_{ab} a(ij,ab) c_{\mu i} c_{\nu j} c_{\sigma a} c_{\rho b} \tag{23}$$

$$L'^{(2)}_{pi} = \sum_j \sum_{ab} a(ij,ab) \langle pj \| ab \rangle + \sum_{jk} K'^{(2)}_{jk} A_{pijk} + \sum_{ab} K''^{(2)}_{ab} A_{piab} \tag{24}$$

$$L''^{(2)}_{pa} = \sum_{ij} \sum_b a(ij,ab) \langle ij \| pb \rangle \tag{25}$$

$$K'^{(2)}_{ij} = -(1/2)\sum_k \sum_{ab} a(ik,ab) a(jk,ab) \tag{26}$$

$$K''^{(2)}_{ab} = (1/2)\sum_{ij}\sum_c a(ij,ac) a(ij,bc) \tag{27}$$

the energy gradient can be written as

$$\mathrm{d}E(\mathrm{MP2})/\mathrm{d}\lambda = \sum_{\mu\nu\sigma\rho} \partial \langle \mu\nu \| \sigma\rho \rangle / \partial\lambda T^{(2)}_{\mu\nu\sigma\rho} + \sum_a \sum_i [U^{\lambda}_{ai} L'^{(2)}_{ai} + U^{\lambda}_{ia} L''^{(2)}_{ia}]$$
$$- (1/2)\sum_{ij} S^{\lambda}_{ij} [L'^{(2)}_{ij} + (\epsilon_i + \epsilon_j) K'^{(2)}_{ij}] + \sum_{ij} F^{(\lambda)}_{ij} K'^{(2)}_{ij}$$
$$- (1/2)\sum_{ab} S^{\lambda}_{ab} [L''^{(2)}_{ab} + (\epsilon_a + \epsilon_b) K''^{(2)}_{ab}] + \sum_{ab} F^{(\lambda)}_{ab} K''^{(2)}_{ab} \tag{28}$$

The unknown U^{λ}_{ia} can be eliminated using eqn. (16), thus leading to

$$\sum_a \sum_i [U^{\lambda}_{ai} L'^{(2)}_{ai} + U^{\lambda}_{ia} L''^{(2)}_{ia}] = \sum_a \sum_i U^{\lambda}_{ai} [L'^{(2)}_{ai} - L''^{(2)}_{ia}] - \sum_a \sum_i S^{\lambda}_{ai} L''^{(2)}_{ia} \tag{29}$$

Furthermore, the unknown U^{λ}_{ai} can be eliminated with the aid of the z-vector method of Handy and Schaefer [20]

$$\sum_b \sum_j [A_{bjai} + (\epsilon_a - \epsilon_i)\delta_{ij}\delta_{ab}] Z_{bj} = (L'^{(2)}_{ai} - L''^{(2)}_{ia}) \tag{30}$$

leading to

$$\sum_a \sum_i (L'^{(2)}_{ai} - L''^{(2)}_{ia}) U^{\lambda}_{ai} = \sum_b \sum_j B^{(\lambda)}_{bj} Z_{bj} \tag{31}$$

Using eqns. (29) and (31) and transforming all terms from the MO to the AO representation, the MP2 energy gradient can be written

$$\mathrm{d}E(\mathrm{MP2})/\mathrm{d}\lambda = \sum_{\mu\nu\sigma\rho} T^{(2)}_{\mu\nu\sigma\rho} \partial \langle \mu\nu \| \sigma\rho \rangle / \partial\lambda +$$
$$\sum_{\mu\nu} F^{(\lambda)}_{\mu\nu} P^{(2)}_{\mu\nu} + \sum_{\mu\nu} S^{\lambda}_{\mu\nu} W^{(2)}_{\mu\nu} \tag{32}$$

with

$$P^{(2)}_{\mu\nu} = \sum_{pq} c_{\mu p} c_{\nu q} N^{(2)}_{pq} - (1/2) \sum_i \sum_a Z_{ai} (c_{\mu a} c_{\nu i} + c_{\mu i} c_{\nu a}) \tag{33}$$

$$N^{(2)}_{pq} = \begin{cases} K'_{ij} & p=i, q=j \\ K''_{ab} & p=a, q=b \\ 0 & \text{otherwise} \end{cases} \tag{34}$$

$$W^{(2)}_{\mu\nu} = \sum_{pq} c_{\mu p} c_{\nu q} M^{(2)}_{pq} + (1/2) \sum_i \sum_a Z_{ai} \epsilon_i (c_{\mu a} c_{\nu i} + c_{\mu i} c_{\nu a}) + (1/2) \sum_{ijk} \sum_a c_{\mu i} c_{\nu j} Z_{ak} A_{akij} \tag{35}$$

$$M^{(2)}_{pq} = \begin{cases} -(1/2)[L'_{ij} + (\epsilon_i + \epsilon_j) K'_{ij}] & p=i, q=j \\ -(1/2)[L''_{ab} + (\epsilon_a + \epsilon_b) K''_{ab}] & p=a, q=b \\ -(1/2) L''_{ia} & p=i, q=a \\ -(1/2) L''_{ia} & p=a, q=i \end{cases} \tag{36}$$

Equation (32) reveals that the MP2 energy gradient depends on the derivatives of the two-electron integrals, the one-electron integrals (since $F^{(\lambda)}_{\mu\nu}$ depends on the derivatives of the core hamiltonian and those of the two-electron part), and the overlap integrals, all expressed in terms of basis functions. The factors $T^{(2)}_{\mu\nu\sigma\rho}$, $P^{(2)}_{\mu\nu}$, and $W^{(2)}_{\mu\nu}$ do not depend on the perturbation λ and therefore contain no derivatives. They can be calculated using the orbital energies, coefficients of the HF wave function, the components of the z-vector and certain double bar integrals. Note that $T^{(2)}$ is not needed to calculate response densities or any other response property.

The equations that determine $P^{(2)}_{\mu\nu}$, $T^{(2)}_{\mu\nu\sigma\rho}$, and $W^{(2)}_{\mu\nu}$ can be generalized for use at higher order of MP perturbation theory with the aid of the four quantities L'_{pi}, L''_{pa}, K'_{ij}, K''_{ab} that determine M_{pq} and N_{pq}. Also, the formulas can be extended to QCI theory [21] as will be shown elsewhere [22]. It is possible to write the expression for the analytical MPn and QCI energy gradient in the following way [22].

$$dE(\text{Method})/d\lambda = \sum_{\mu\nu\sigma\rho} T^{(\text{Method})}_{\mu\nu\sigma\rho} \partial \langle \mu\nu \| \sigma\rho \rangle / \partial\lambda + \sum_{\mu\nu} F^{(\lambda)}_{\mu\nu} P^{(\text{Method})}_{\mu\nu} + \sum_{\mu\nu} S^{\lambda}_{\mu\nu} W^{(\text{Method})}_{\mu\nu} \tag{37}$$

In eqn. (37), $P_{\mu\nu}$ represents a generalized density matrix, namely the response density matrix. Similarly, $T_{\mu\nu\sigma\rho}$ can be regarded as a two-particle density matrix and $W_{\mu\nu}$ as generalized energy weighted density matrix.

Using

$$P^{(\text{Method})}_{\mu\nu} = \sum_{pq} c_{\mu p} c_{\nu q} N^{(\text{Method})}_{pq} - (1/2) \sum_i \sum_a Z_{ai} (c_{\mu a} c_{\nu i} + c_{\mu i} c_{\nu a}) \tag{38}$$

and the z-vector method, it is possible to calculate the response density matrix at little extra cost once $E^{(\text{Method})}$ has been calculated at the MPn or QCI level of theory. If, however, a geometry optimization is performed, then the response

density matrix is automatically calculated at no extra cost, as is revealed by eqn. (37).

The response density matrix can be analyzed in various ways. One can diagonalize $\boldsymbol{P}^{\mathrm{Res}}$ to get natural orbitals and their occupation numbers. Also, one can use the response density matrix directly to carry out a Mulliken population analysis [23] or to investigate the response density distribution with a topological analysis or with the virial partitioning method [24]. Correlation effects might be investigated and visualized by calculating $\boldsymbol{P}^{\mathrm{cor}}=\boldsymbol{P}^{\mathrm{Res}}-\boldsymbol{P}^{\mathrm{SCF}}$. The Mulliken population analysis of $\boldsymbol{P}^{\mathrm{cor}}$ reveals the changes in orbital populations due to correlation corrections. It is straightforward to discuss these changes in terms of left–right, in–out, and angular correlation effects.

In the following section, we present response properties calculated with eqns. (8) and (38) at the MPn ($n=2,3,4$) [2–5], CCD [25], QCISD, and QCISD(T) level of theory [9].

RESULTS

Response properties of 20 molecules are investigated at nine different levels of theory using the ab initio program COLOGNE [26]. Two basis sets have been employed, namely the 6-31G(d,p) [27] and 6-311G(2d,2p) [28(a)] ((12s9p2d)[621111,52111,11] abbreviated as MC-311G(2d) for second row atoms [28(b)]) basis sets that are of VDZ+P and VTZ+2P quality. These basis sets are used in routine investigations and it is therefore of interest to see how accurate response properties calculated with the 6-31G(d,p) and 6-311G(2d,2p) (or MC-311G(2d,2p)) basis set are.

In Table 1, some results for carbon monoxide are summarized. Response properties of CO, in particular its dipole moment, are sensitive to both basis set and correlation effects and therefore CO has been used in many investigations as an appropriate test molecule [29–31]. Calculated response electron density distributions and difference response electron density distributions for CO are shown in Figs. 1–7. The computed atomic charges and the molecular dipole moment of CO are analyzed in Figs. 8 and 9. Figure 10 gives a section of the dipole moment curve of CO calculated at various levels of theory.

In Table 2, response properties (atomic charges, dipole moments, and quadrupole moments) of various small molecules calculated at MP2 geometries with the 6-31G(d,p) basis are summarized. A similar set of data obtained with the 6-311G(2d,2p) or MC-311G(2d,2p) basis is given in Table 3.

We will analyze in the next section the results obtained for CO in some detail.

INVESTIGATION OF THE RESPONSE PROPERTIES OF CARBON MONOXIDE

In Fig. 1, the difference electron density distribution $\Delta\rho(\mathbf{r})^{\mathrm{res}}(\mathrm{MP2})=\rho(\mathbf{r})^{\mathrm{res}}(\mathrm{MP2})-\rho(\mathbf{r})^{\mathrm{HF}}$ of CO is given in the form of a contour line diagram

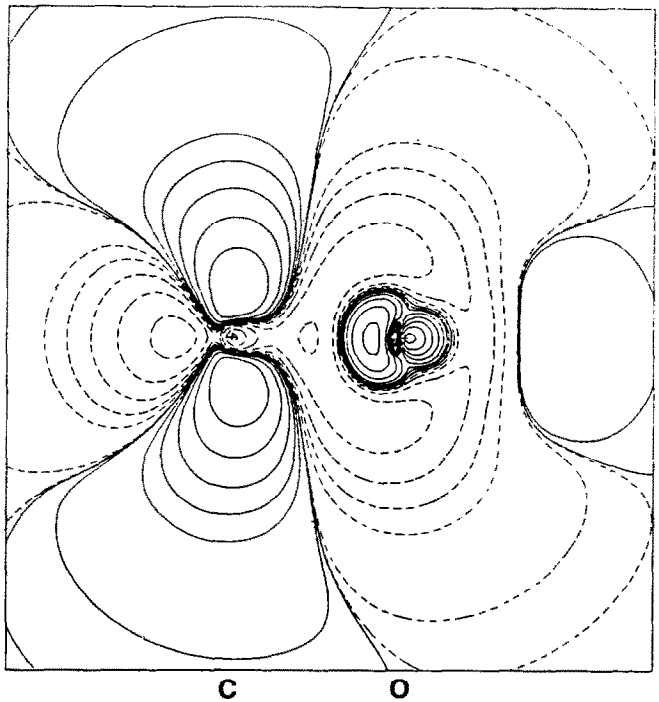

Fig. 1. Contour line diagram of the difference electron density distribution $\Delta\rho(\mathbf{r})^{res}(MP2) = \rho(\mathbf{r})^{res}(MP2) - \rho(\mathbf{r})^{HF}$ of CO calculated with the 6-311G(2d) basis. Solid (dashed) contour lines are in regions of positive (negative) difference densities. The positions of the C and the O nucleus are indicated. In this and the following figures, contour levels of 10^{-2}, 0.66×10^{-2}, 0.33×10^{-2}, 10^{-3}, 0.66×10^{-3}, 0.33×10^{-3}, etc. e/Å^3 have been used.

where $\rho(\mathbf{r})^{res}(MP2)$ is the response density distribution calculated at the MP2 level with the 6-311G(2d) basis and $\rho(\mathbf{r})^{HF}$ is the corresponding HF density distribution obtained for the same geometry with the same basis set, i.e. $\Delta\rho(\mathbf{r})^{res}(MP2)$ gives the correlation corrections determined at the MP2 level. As noted above, the easiest way to determine $\Delta\rho(\mathbf{r})^{res}(MP2)$ is to calculate $\boldsymbol{P}^{cor}$ and the corresponding changes in the natural orbitals. Solid (dashed) contour lines are in regions of positive (negative) difference densities.

Obviously, correlation corrections at the MP2 level lead to a transfer of negative charge from the oxygen atom to the carbon atom. According to Mulliken population values, the atomic charge of the O (C) atom decreases (increases) by 60% relative to the HF value. This means that, at the HF level, the polarity of the CO bond is largely overestimated, leading to relatively large errors in atomic charges and dipole moment of CO. The latter changes its sign due to correlation corrections by -0.5 Debye (see Fig. 10). Since the MP2 value of the CO bond length, R(CO), is longer than its HF value (Table 1), there is

TABLE 1

Calculated bond length, atomic charge, and dipole moment of carbon monoxide[a]

Method	R(CO)	q(C)	μ
Basis: 6-31G(d)			
HF	1.114	268	0.265
MP2	1.150	137	−0.192
MP3	1.134	182	0.020
MP4(DQ)	1.146	173	0.003
MP4(SDQ)	1.146	171	−0.017
MP4(SDTQ)	1.158	158	−0.088
CCD	1.138	177	0.019
QCISD	1.145	177	0.011
QCISD(T)	1.148	171	−0.016
Basis: 6-311G(2d)			
HF	1.103	232	0.122
MP2	1.136	93	−0.306
MP3	1.120	139	−0.120
MP4(DQ)	1.124	128	−0.133
MP4(SDQ)	1.131	124	−0.155
MP4(SDTQ)	1.144	110	−0.237
CCD	1.124	133	−0.119
QCISD	1.129	130	−0.130
QCISD(T)	1.134	123	−0.164
Exptl.	1.128	(145)[b]	−0.112

[a]CO bond length in Å, atomic charge in melectron, dipole moment, μ, in Debye.
[b]Derived from calculated R, q, and μ values using the equation: $\mu = a[qR(\mathrm{CO})] + b$.

also a geometry effect of 0.1 Debye that influences the MP2 dipole moment. Thus, the actual MP2 correlation correction is −0.4 Debye (Table 1).

This basic failure of HF theory is well known and has been documented in the case of the CO molecule many times [29–32]. Figure 1 reveals more details of the correlation correction of the electron density distribution at the MP2 level. The charge transfer from O to C predominantly takes place in the space of the π-electrons and is connected with left–right correlation of π-electrons. In addition to the transfer of π-electrons from O to C, there seems to be also a transfer of electronic charge from C to O taking place both in the inner valence region and in the outer regions that are primarily described by the polarization functions (see Fig. 1). In both cases, the charge transfer seems to involve σ orbitals.

A detailed analysis of the MP2 correlation corrections of the orbital populations reveals that the transfer of π charges decreases the atomic charge of O by 61% (0.162 e), but increases the atomic charge of C by 68% (0.179 e). The difference is due to changes in the σ populations involving s, $p\sigma$, and d basis

functions. For example, σ-charge at C is transferred from the inner to the outer valence region due to in–out correlation. Some of this charge may also be transferred to the π-orbitals as a result of angular correlation. Alternatively, the increase of negative charge in the π-orbitals at C may stem from the outer σ-region of O (combination of left–right and angular correlation), which is depopulated relative to the charge distribution obtained at the HF level. In total, the charge distribution at O decreases and contracts while that at C increases and expands (Fig. 1). Since the O nucleus is deshielded, it can bind some diffuse charge in the lone pair region that seems to be lost by the C atom (Fig. 1). According to Mulliken population values, there is a transfer of 0.014 e from the d basis functions at C to those at O.

Clearly, left–right correlation dominates correlation corrections at the MP2 level and, therefore, a characteristic lengthening of the CO bond length is calculated at this level of theory (Table 1). Less important, but substantial, are angular and in–out correlations.

Similar correlation corrections to the electron density distribution are found at all levels of theory performed in this work, i.e. at the MP3, MP4(DQ),

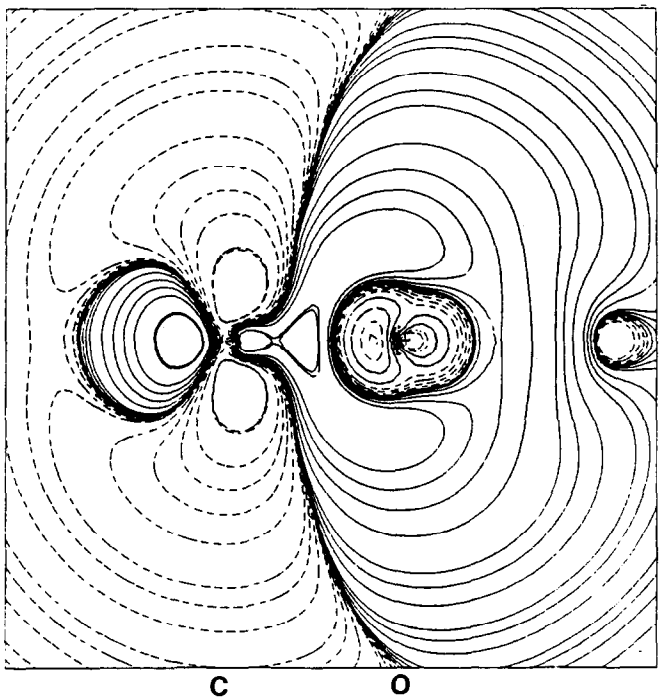

Fig. 2. Contour line diagram of the difference electron density distribution $\Delta\rho(\mathbf{r})^{res}(\mathrm{MP3}) = \rho(\mathbf{r})^{res}(\mathrm{MP3}) - \rho(\mathbf{r})^{res}(\mathrm{MP2})$ of CO calculated with the 6-311G(2d) basis. Solid (dashed) contour lines are in regions of positive (negative) difference densities. The positions of the C and the O nucleus are indicated.

MP4(SDQ), MP4(SDTQ), CCD, QCISD, and QCISD(T) levels. Qualitatively, there are no differences in the corresponding response densities, which means that MP2 already leads to the most important correlation corrections. In order to find out about the different correlation effects covered by the various methods, difference response density plots have to be investigated.

In Figure 2, the difference response electron density $\Delta\rho^{res}(MP3) = \rho^{res}(MP3) - \rho^{res}(MP2)$ is shown. It reveals that the MP3 correlation corrections decrease MP2 effects, i.e. the MP3 response density distribution is between the MP2 and the HF electron density distribution. Changes at the MP3 level relative to those calculated at MP2 comprise a π electron transfer from C to O, transfer of σ electrons from outer valence functions to inner valence functions at C and vice versa at O as well as changes in the diffuse charge distribution in the lone pair regions of C and O. These changes lead to an increase of the CO bond polarity and increased atomic charges relative to MP2. The MP3 value of the CO dipole moment is about the average of the HF and MP2 dipole moments and, thereby, it comes close to the experimental value (see Table 1). This, of course, is due to a fortuitous cancellation of errors.

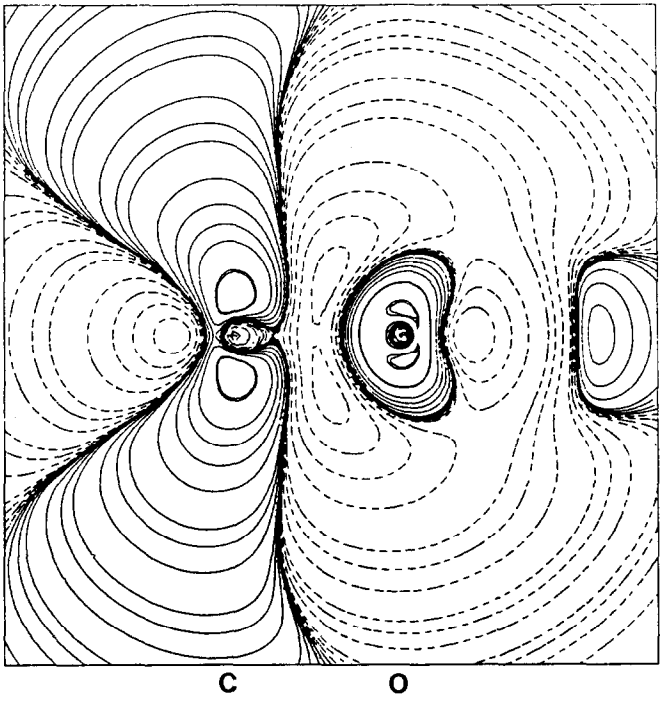

Fig. 3. Contour line diagram of the difference electron density distribution $\Delta\rho(\mathbf{r})^{res}(MP4(SDQ)) = \rho(\mathbf{r})^{res}(MP4(SDQ)) - \rho(\mathbf{r})^{res}(MP3)$ of CO calculated with the 6-311G(2d) basis. Solid (dashed) contour lines are in regions of positive (negative) difference densities. The positions of the C and the O nucleus are indicated.

Clearly, at MP3 the correlation effects of the double excitations are reduced relative to those calculated at the MP2 level. As has been outlined before, this is due to the fact that, at MP3, coupling between double excitations is introduced and therefore correlation between two electrons is no longer independent of the correlation of the other electron pairs. At MP2, only the interactions of the double excitations with the ground state wave function is calculated and, as a consequence, electron pair correlation is overestimated.

In Figure 3, the difference response density $\Delta\rho^{res}(MP4(SDQ)) = \rho^{res}(MP4(SDQ)) - \rho^{res}(MP3)$ is given. Its general features are similar to those of $\Delta\rho^{res}(MP2)$ (Fig. 1), which means that MP4(SDQ) correlation corrections are in the same direction as MP2 correlation corrections. As a consequence, correlation corrections to charges, dipole moment, and other molecular properties are larger than those calculated at the MP3 level of theory. However, they are still smaller than those calculated at the MP2 level as is reflected by Fig. 4, which shows the difference response density $\rho^{res}(MP4(SDQ)) - \rho^{res}(MP2)$. Again, the pattern of changes is very similar to that obtained at the MP3 level. Obviously, corrections due to single, double

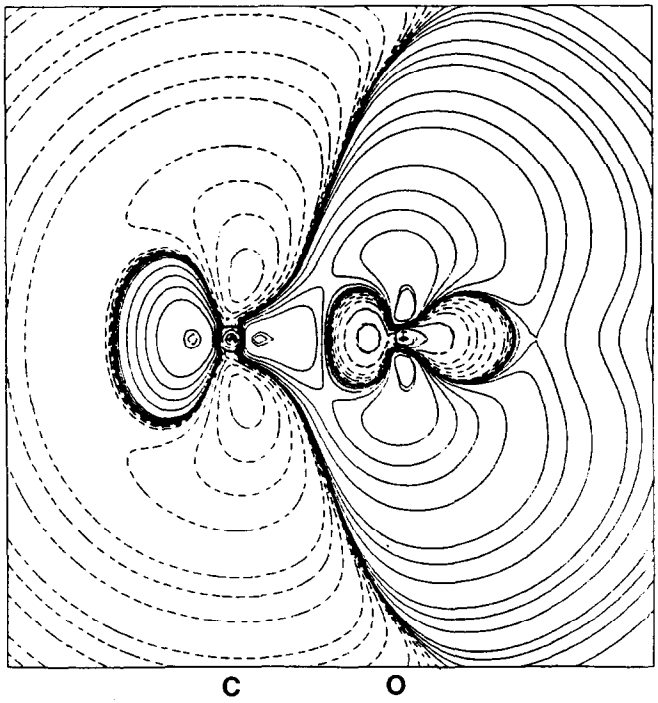

Fig. 4. Contour line diagram of the difference electron density distribution $\rho(\mathbf{r})^{res}(MP4(SDQ)) - \rho(\mathbf{r})^{res}(MP2)$ of CO calculated with the 6-311G(2d) basis. Solid (dashed) contour lines are in regions of positive (negative) difference densities. The positions of the C and the O nucleus are indicated.

and quadruple excitations at the MP4 level are between those obtained at the MP2 and the MP3 level.

Figure 5 shows the changes in the response density distribution that are due to triple excitations at the MP4 level of theory. They enhance those effects that result from S, D, and Q excitations at MP4, i.e. they increase the charge transfer from the O to the C atom. An analysis of calculated charges and dipole moments shows that the changes due to triples are of the same magnitude as those of the S, D, and Q excitations together, thus stressing the importance of the triple excitations at the MP4 level.

When going from MP4(SDTQ) to QCISD(T), correlation corrections change back into the direction of MP3 results. This is illustrated by Fig. 6, which shows the difference response density distribution $\Delta\rho^{res}(\mathrm{QCISD(T)}) = \rho^{res}(\mathrm{QCISD(T)}) - \rho^{res}(\mathrm{MP4(SDTQ)})$. Again, there is a transfer of π-charge back to the O atom accompanied by a smaller transfer of σ-charge from the inner valence region of O to the lone pair region of C. These changes suggest that left–right correlation at the MP4 level is still exaggerated to some extent.

Triple excitations at the QCI level have the same effect as triple excitations

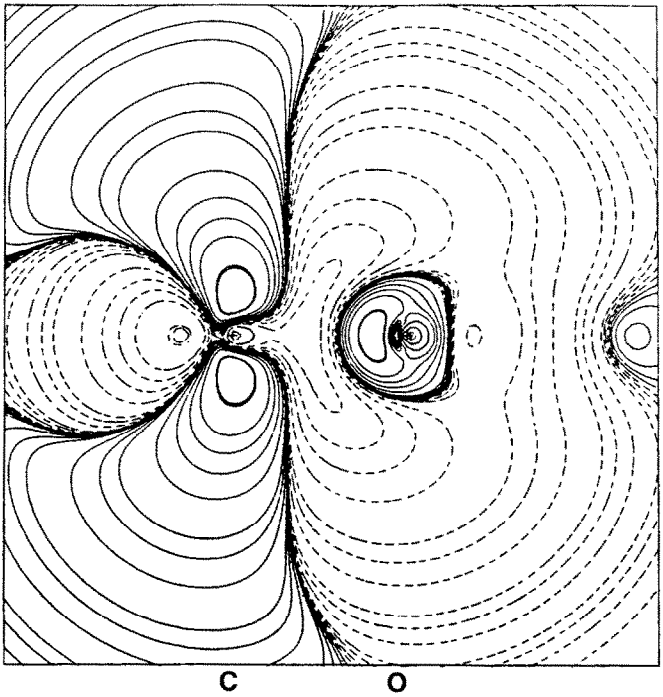

Fig. 5. Contour line diagram of the difference electron density distribution $\Delta\rho(\mathbf{r})^{res}(\mathrm{MP4(SDQT)}) = \rho(\mathbf{r})^{res}(\mathrm{MP4(SDQT)}) - \rho(\mathbf{r})^{res}(\mathrm{MP4(SDQ)})$ of CO calculated with the 6-311G(2d) basis. Solid (dashed) contour lines are in regions of positive (negative) difference densities. The positions of the C and the O nucleus are indicated.

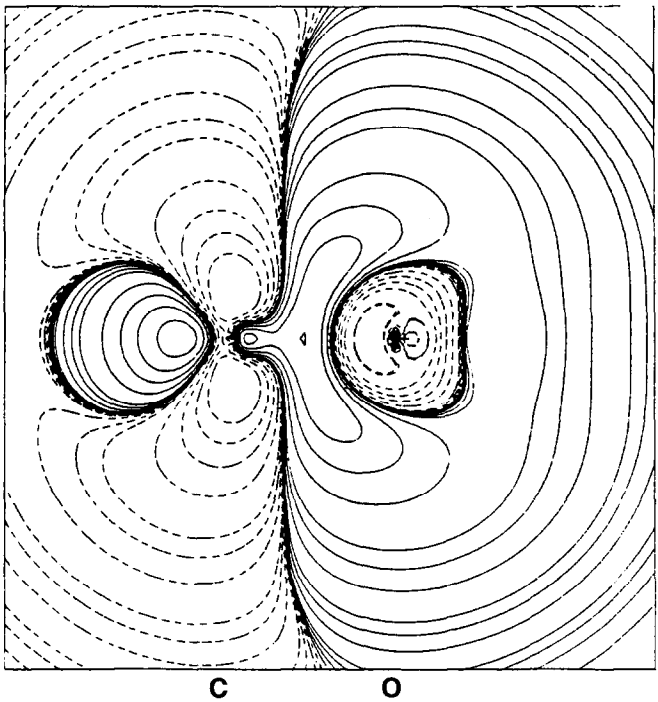

Fig. 6. Contour line diagram of the difference electron density distribution $\Delta\rho(\mathbf{r})^{res}(\mathrm{QCISD(T)}) = \rho(\mathbf{r})^{res}(\mathrm{QCISD(T)}) - \rho(\mathbf{r})^{res}(\mathrm{MP4(SDQT)})$ of CO calculated with the 6-311G(2d) basis. Solid (dashed) contour lines are in regions of positive (negative) difference densities. The positions of the C and the O nucleus are indicated.

at the MP4 level (see Fig. 7). They increase (decrease) the negative charge at C (O), thus also making the CO dipole moment more negative (Table 1).

The data of Table 1 and the diagrams in Figs. 8 and 9 provide a basis to analyze correlation effects on a more quantitative basis. The major conclusions drawn from this analysis can be summarized as follows.

(1) The largest part of the correlation corrections is recovered at MP2, but higher-order effects are still considerable and cannot be neglected. Often, but not always, the values of the calculated response properties at higher levels of correlation theory (MP4, QCI, etc.) are between those obtained at the HF and MP2 levels.

(2) Correlation corrections due to D excitations are exaggerated at the MP2 level. They are reduced at the MP3 or CCD level of theory where coupling between D excitations is introduced.

(3) Single excitations do not change the values of response properties significantly. In most cases they are not very important for obtaining accurate response properties. This is opposite to the observations made when calculating one-electron properties as expectation values at the CI level [29,32]. There,

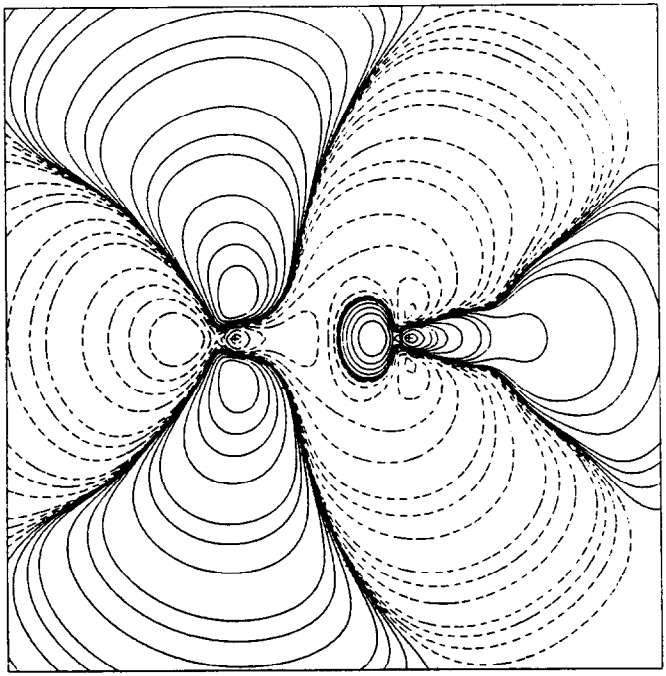

Fig. 7. Contour line diagram of the difference electron density distribution $\rho(\mathbf{r})^{res}(\mathrm{QCISD(T)}) - \rho(\mathbf{r})^{res}(\mathrm{QCISD})$ of CO calculated with the 6-311G(2d) basis. Solid (dashed) contour lines are in regions of positive (negative) densities. The positions of the C and the O nucleus are indicated.

S excitations are important to account for orbital relaxation effects. However, these effects are implicitly considered when solving the CPHF equations (or the corresponding **z**-vector equation) within the energy derivative approach.

(4) The influence of T excitations at MP4 is as large as the influence of S, D, and Q excitations together, at least for molecules with multiple bonds. Similar observations are made for the T corrections at the QCI level of theory. However, it seems that T excitations at MP4 are to some extent exaggerated for the same reason as D excitations are exaggerated at MP2.

As Figs. 8 and 9 clearly show, there is an oscillation in the correlation corrections to CO charges and CO dipole moment [29–32]. Oscillations are almost parallel when different basis sets are used (6-31G(d) and 6-311G(2d), see Figs. 8 and 9). This is in line with published results on the CO dipole moment. Available data suggest that, for larger basis sets, CO charges are shifted to lower values and more negative dipole moments. Hence, typical features of correlation corrections at the various levels of theory are correctly recovered when using relatively small basis sets such as a VDZ+P basis set.

For small and medium-sized basis sets, accurate one-electron properties can

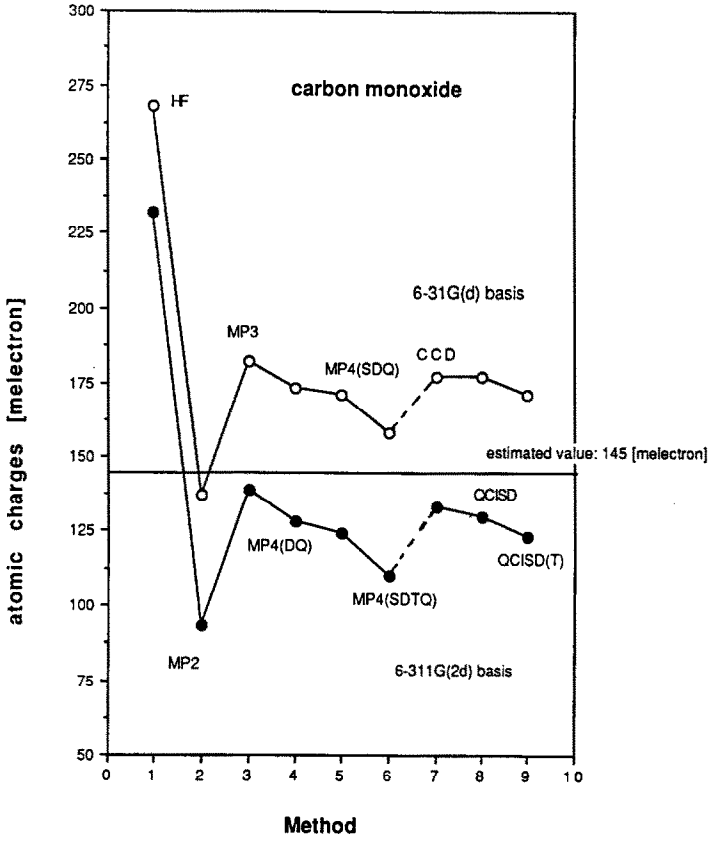

Fig. 8. Dependence of calculated carbon charge of carbon monoxide on method and basis set.

only be expected if there is a fortuitous cancellation of errors. For CO, this seems to be the case at the MP2/6-31G(d) and MP4(SDTQ)/6-31G(d) levels of theory. With the larger 6-311G(2d) basis set, cancellation of errors leads to MP3 and CCD values close to the experimental values. These observations can be used when doing routine calculations with these basis sets (see below) or when analyzing published data. For example, CCSD/DZP and CCSDT/DZP values of the CO dipole moment [31] are close to its experimental value (−0.112 Debye; for experimental dipole moments, see ref. 33) because the basis set chosen leads to values between those obtained with the 6-31G(d) and the 6-311G(2d) basis sets (Figs. 8 and 9). Since the CCSD and CCSDT results are parallel to the corresponding QCI results, agreement with the experimental CO dipole moment is obtained. A CCSD/TZP calculation [31] gives a very accurate prediction of μ(CO) as does the QCISD/6-311G(2d) used in this work. Accordingly, CCSDT/TZP should shift the dipole moment below the experi-

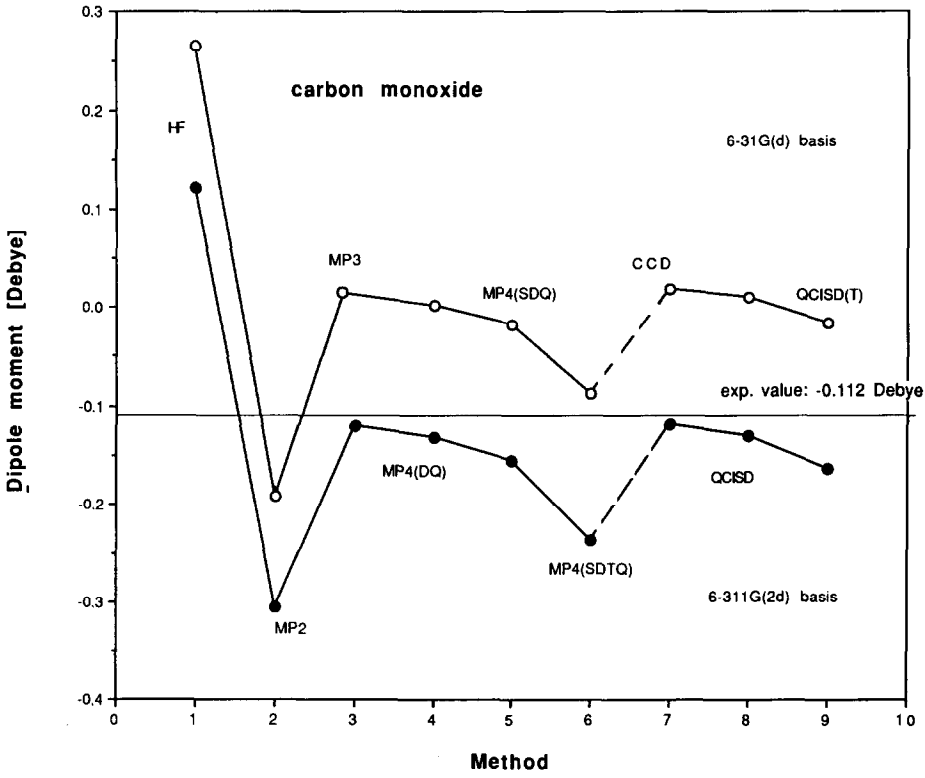

Fig. 9. Dependence of calculated dipole moment of carbon monoxide on method and basis set.

mental value as experienced in this work when using QCISD(T)/6-311G(2d) (see Fig. 9).

The fortuitous cancellation of basis set and correlation errors at the MP3/ and CCD/6-311G(2d) level of theory can be used to get a reasonable description of the CO dipole moment curve close to the equilibrium value. A section of this curve calculated at various levels of theory is shown in Fig. 10. Beside the MP3 and the CCD curves, the calculated QCISD(T) dipole moment curve should also be close to the true one. The MP2 curve, however, is shifted to values of μ that are too negative.

It can also be seen from Fig. 10 that the HF dipole moment curve is shifted in a direction opposite to that of the MP2 curve, i.e. the HF dipole moment of CO becomes negative only for bond lengths 0.05 Å smaller than the experimental value of 1.128 Å. Also, the descent of the HF dipole moment curve is much steeper than that of the MP3 or CCD curve. However, these features of the HF dipole moment curve are also observed for other molecules (see below) and, hence, the HF description of the CO dipole moment is in no way different from that of other molecules. It is only that, for CO, the magnitude of the

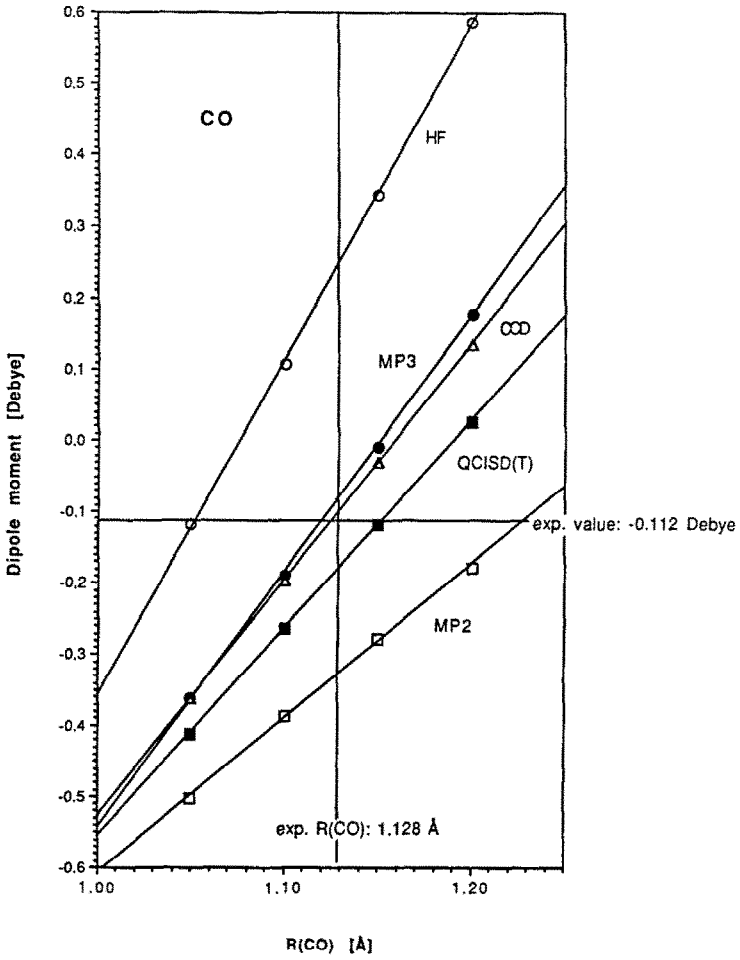

Fig. 10. Section of the calculated dipole moment curves of carbon monoxide.

equilibrium dipole moment is similar to the magnitude of the correlation corrections and therefore HF and correlation corrected methods lead to values of the dipole moment differing in sign.

One of the pending problems in quantum chemistry is the question whether MP4 calculations provide a reliable estimate of correlation effects. It is clear that this is not the case if non-dynamical correlation effects become important when calculating molecular energies [34]. Calculations carried out for dissociation reactions of small molecules suggest that MPn methods converge very slowly [34]. Nevertheless, there is a general belief that MP4 can recover at least most of the dynamical correlation effects for molecules in their equilibrium geometries.

Although the MP4 level is as far as we can go in this work (for recent MP5

	CCD	QCISD	QCISD(T)	
E(MP2)	yes	yes	yes	D
E(MP3)	yes	yes	yes	D
		yes	yes	S
	yes	yes	yes	D
E(MP4)	yes	yes	yes	Q
			yes	T
		yes	yes	SS
	yes	yes	yes	DD
	(yes)	(yes)	(yes)	QQ
				TT
E(MP5)		y, y	y, y	SD, DS
	y, y	y, y	y, y	DQ, QD
			y, y	ST, TS
			y, y	DT, TD
				TQ, QT

Scheme 1. Analysis of CCD, QCISD, and QCISD(T) in terms of MPn methods with $n<6$. For each method it is indicated by yes (abbreviated y) whether a particular energy contribution arising from single (S), double (D), triple (T), quadrupole excitations (Q) at MPn (with $n=2, 3, 4, 5$) is fully contained. If the energy contribution is only partially contained, the yes is put in parentheses.

calculations, see ref. 35), CC and QCI methods provide a basis for predicting changes in correlation corrections at higher levels of perturbation theory.

As indicated in Scheme 1, CCD recovers *D* and *Q* excitation effects at MP4 as well as *DD*, *DQ*, and partially *QQ* effects at MP5. QCISD comprises, in addition, the effects of *S* excitations at MP4 and those of *SS* and *SD* excitations at MP5. If *T* excitations are included at the QCI level, then QCI is correct at fourth-order perturbation theory and recovers apart from *TT* and *TQ* effects all other excitation effects at fifth-order perturbation theory [10]. Hence, both CC and QCI methods give an indication how fifth-order perturbation will change correlation corrections.

The CCD and QCI results obtained for CO suggest that considerable changes have to be expected for MP5, possibly correcting the MP4 response density back into the direction of the MP3 response density. It is reasonable to predict that oscillation of correlation corrections will continue at MP5 and MP6, probably only slowly damping out at higher orders of perturbation theory. This

suggests that, for high quality correlation descriptions, neither MP4 nor MP5 will be sufficient. With the VTZ+2P basis set, the MP5 results of CO will probably be closer to experimental values than the MP4 results, but the opposite may be true when employing a different basis set. QCI methods, which also contain, in addition to fifth-order contributions, important infinite-order contributions [36], seem to converge faster to a limit value if *D*, *S*, *T*, etc. excitations are gradually introduced. At least this is suggested by the data collected in this work.

RESPONSE PROPERTIES OF SOME ONE- AND TWO-HEAVY ATOM SYSTEMS

It is well-known that an accurate calculation of dipole moments requires *sp*-saturated basis sets with polarization functions. Quadrupole moments and octopole moments require even more accurate basis sets comprising also diffuse functions. In general, multipole moments of molecules constituted from first and second row elements should be calculated with extended basis sets that contain polarization functions with $l=m+1$ where l is the angular quantum number and m is the order of the multipole moment. Also, the exponents of added diffuse functions should decrease with an increase in m since higher multipole moments become more sensitive to diffuse charge distributions.

It is also known that basis set errors in the calculation of one-electron properties cannot be recovered by including correlation effects in the calculation. So far, the results we have obtained for CO with the 6-311G(2d) basis set suggest that the basis set used is still too small and leads to significant basis set errors. The available data from the literature confirm this point [29–32]. However, it is not the goal of this work to calculate highly accurate one-electron properties, but to investigate and predict correlation effects that can occur at higher levels of theory. As discussed above and reflected by Figs. 8 and 9, these effects can already be found when using a VDZ+P basis set.

In Table 2, MP2, MP4(SDQ), and QCISD correlation corrections for atomic charges, dipole moments, and quadrupole moments of some selected molecules are given. They have been calculated with the 6-31G(d,p) basis set at MP2 geometries [37], which are sufficiently close to experimental values to eliminate larger geometry effects in calculated properties. The following observations can be made when analyzing the data of Table 2.

(1) Relative correlation corrections are largest for charges, smaller for dipole moments and smallest for quadrupole moments. This observation, however, may change for larger basis sets.

(2) Relative correlation corrections are larger for covalently bonded molecules than for ionic molecules. Also, they are larger for molecules with multiple bonds than those with just single bonds. The largest effects are found for molecules with semipolar bonds.

(3) For ionic species, MP and QCI corrections are essentially the same.

TABLE 2

HF values and correlation corrections obtained for atomic charges, dipole moments, and quadrupole moments at various levels of theory with the 6-31G(d,p) basis set[a]

Molecule	Charges	Dipole	Quadrupole
CO (1.150) (O; xx=yy, zz)[b]			
HF	−302	0.44	−9.97; −12.10
MP2	169	−0.63	−0.05; 0.01
MP4(SDQ)	133	−0.44	−0.01; 0.04
MP4(SDQT)	154	−0.54	−0.01; 0.02
QCISD	125	−0.41	−0.01; 0.04
QCISD(T)	135	−0.45	−0.02; 0.05
HCP (1.560, 1.070) (C, P; xx=yy, zz)			
HF	−335; 135	0.73	−19.96; −15.56
MP2	97; −55	0.01	0.43; −0.45
MP4(SDQ)	76; −36	−0.10	0.40; −0.37
QCISD	71; −32	−0.11	0.41; −0.40
PH_3 (1.405, 94.5) (P; xx=yy, zz)			
HF	+162	−0.86	−14.74; 17.14
MP2	−54	−0.05	0.04; 0.16
MP4(SDQ)	−30	+0.01	0.02; 0.24
QCISD	−27	+0.02	0.02; 0.25
ClF (1.659) (F; xx=yy, zz)			
HF	−359	1.33	−17.22; −15.76
MP2	54	−0.25	−0.10; 0.08
MP4(SDQ)	45	−0.21	−0.07; 0.03
QCISD	44	−0.20	−0.07; 0.03
H_2S (1.329, 92.8) (S; xx-σ_v, yy-$\sigma_{v'}$, zz-C_2)			
HF	−132	1.38	−16.70; −12.30; −13.74
MP2	−7	−0.01	0.06; −0.03; 0.04
MP4(SDQ)	16	−0.08	0.12; −0.07; 0.03
QCISD	17	−0.08	0.12; −0.08; 0.03
HCl (1.268) (Cl; xx=yy, zz)			
HF	−192	1.47	−13.99; −10.41
MP2	9	−0.05	0.03; −0.08
MP4(SDQ)	21	−0.10	0.05; −0.14
QCISD	22	−0.10	0.05; −0.14

TABLE 2 (continued)

Molecule	Charges	Dipole	Quadrupole
NH_3 (1.011, 106.1) (N; xx=yy, zz)			
HF	−786	1.92	−6.10; −8.80
MP2	37	−0.05	−0.08; −0.04
MP4(SDQ)	54	−0.07	−0.09; −0.01
QCISD	56	−0.07	−0.09; −0.01
FH (0.921) (F; xx=yy, zz)			
HF	−397	1.98	−5.38; −3.32
MP2	20	−0.10	−0.07; −0.14
MP4(SDQ)	24	−0.10	−0.07; −0.14
QCISD	24	−0.11	−0.07; −0.14
H_2O (0.961; 103.9) (O; xx-σ_v, yy-$\sigma_{v'}$, zz-C_2			
HF	−674	2.20	−7.17; −4.14; −5.93
MP2	32	−0.09	−0.08; −0.15; −0.10
MP4(SDQ)	42	−0.10	−0.05; −0.15; −0.09
QCISD	42	−0.10	−0.05; −0.15; −0.09
CS (1.544) (C; xx=yy, zz)			
HF	−22	1.20	−18.40; −20.50
MP2	−121	0.81	0.46; −0.60
MP4(SDQ)	−111	0.54	0.39; −0.33
MP4(SDQT)	−100	0.63	0.47; −0.47
QCISD	−84	0.48	0.37; −0.27
QCISD(T)	−92	0.52	0.41; −0.32
H_2CO (1.219, 1.099, 122.2) (O, C; xx-σ_v, yy-$\sigma_{v'}$, zz-C_2)			
HF	−452; 245	2.83	−11.55; −11.44; −11.86
MP2	118; −81	−0.60	0.04; −0.27; −0.17
MP4(SDQ)	104; −63	−0.55	0.05; −0.23; −0.17
MP4(SDQT)	115; −68	−0.63	0.06; −0.28; −0.21
QCISD	100; −58	−0.53	0.06; −0.22; −0.18
QCISD(T)	110; −66	−0.60	0.05; −0.25; −0.19
HCN (1.176, 1.064) (N, C; xx=yy, zz)			
HF	−386, 112	3.24	−11.74; −9.47
MP2	80, −35	−0.35	0.25; −0.35
MP4(SDQ)	70, −26	−0.32	0.21; −0.32
QCISD	69, −24	−0.32	0.22; −0.34

TABLE 2 (continued)

Molecule	Charges	Dipole	Quadrupole
LiH (1.623) (Li; xx=yy, zz)			
HF	193	5.94	−5.46; −6.92
MP2	−20	−0.15	−0.12; +0.14
MP4(SDQ)	−40	−0.25	−0.23; +0.22
QCISD	−45	−0.31	−0.29; +0.25
LiF (1.567) (F; xx=yy, zz)			
HF	−661	6.22	−6.96; −0.65
MP2	104	−0.37	−0.48; −0.42
MP4(SDQ)	95	−0.36	−0.46; −0.41
QCISD	92	−0.36	−0.45; −0.41
NaH (1.906) (Na; xx=yy, zz)			
HF	−270	6.89	−8.80; −16.17
MP2	−32	−0.32	−0.25; 0.44
MP4(SDQ)	−58	−0.52	−0.46; 0.72
QCISD	−69	−0.70	−0.60; 0.90
LiCl (2.064) (Cl; xx=yy, zz)			
HF	−499	7.62	−16.43; −1.92
MP2	59	−0.33	−0.17; −0.35
MP4(SDQ)	57	−0.32	−0.16; −0.33
QCISD	56	−0.32	−0.16; −0.32
NaF (1.898) (F; xx=yy, zz)			
HF	−703	7.88	−9.49; −9.44
MP2	101	−0.44	−0.57; −0.04
MP4(SDQ)	95	−0.44	−0.58; −0.08
QCISD	94	−0.47	−0.58; −0.07
NaCl (2.391) (Cl; xx=yy, zz)			
HF	−667	9.50	−19.07; −10.88
MP2	60	−0.37	−0.23; −0.04
MP4(SDQ)	58	−0.35	−0.21; −0.03
QCISD	61	−0.38	−0.23; −0.04

[a]Distances in Å, angles in degrees, charges in melectron, dipole moments in Debye, quadrupole moments in Debye Å.

[b]MP2 geometries are given in the first parentheses. The atoms for which the charges are given, and the quadrupole components are indicated in the second parentheses.

(4) For covalently bonded molecules with just single bonds, MP4(SDQ) and QCISD results are almost identical, in line with the analysis given in Scheme 1. *T* excitations and higher-order effects are not very important and do not change the calculated values significantly.

(5) For molecules with multiple bonds, *T* excitations and higher-order effects become important when evaluating molecular response properties.

(6) If correlation corrections are large, MP2 corrections are usually larger than those obtained at the MP3 and MP4 levels. In cases where correlation corrections are small and/or basis set deficiencies are very large (HCl, H_2S, etc.), MP2 corrections may be smaller than MP4 correlation corrections.

These observations suggest that reasonably accurate response properties for molecules without multiple bonds can already be obtained at the MP2 level provided a sufficiently large basis set is used. This prediction is confirmed by MP2/6-311G(2d,2p) or MP2/MC-311G(2d,2p) values of dipole moments listed in Table 3. Calculated values agree within a few tenths of a Debye with experimental values (see also Fig. 11), even when molecules with multiple bonds are considered. Of course, high accuracy of calculated dipole moments and other response properties is only achieved if MP4(SDTQ) or QCISD(T) and a large basis set is employed. This becomes obvious when considering critical cases such as the CO or CS molecule (see Table 3).

TABLE 3

Comparison of HF/6-311G(2d,2p), MP2/6-311G(2d,2p) and experimental dipole moments[a]

Molecule	HF	MP2	Exptl.
CO	0.34	−0.28	−0.11
HCP	0.44	0.44	0.39
PH_3	0.66	0.60	0.58
CIF	1.32	1.02	0.88
H_2S	1.12	1.08	0.97
HCl	1.24	1.19	1.08
NH_3	1.65	1.59	1.47
FH	1.93	1.81	1.82
H_2O	2.01	1.90	1.85
CS	1.60	2.30	1.98
H_2CO	2.82	2.24	2.34
HCN	3.24	2.91	2.99
LiH	6.06	5.98	5.83
LiF	6.33	6.04	6.28
NaH	7.05	6.72	6.96
LiCl	7.63	7.43	7.12
NaF	8.01	7.65	8.16
NaCl	9.59	9.35	9.00

[a]All values in Debye. The geometries used in the calculations are given in Table 2.

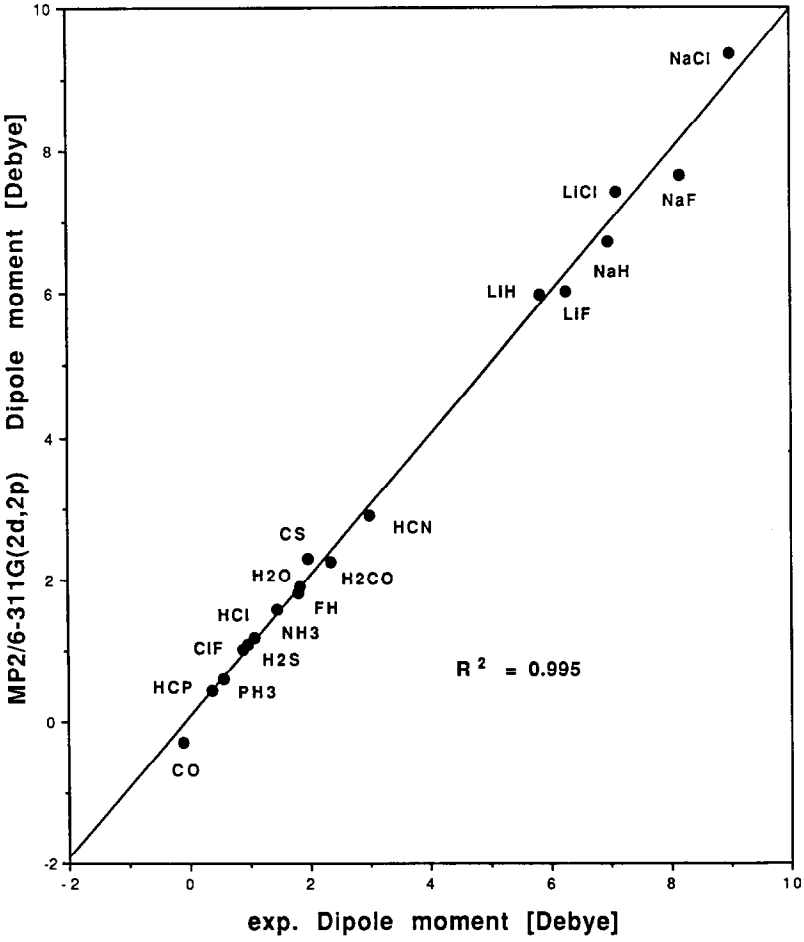

Fig. 11. Comparison of calculated MP2/6-311G(2d,2p) dipole moments with experimental dipole moments.

While it is possible to compute reasonably accurate response properties at relatively low computational costs for single-bonded molecules in their equilibrium geometry, elaborate correlation methods will be needed if a response property is monitored for a variety of internuclear distances far from the equilibrium. In Fig. 12, experimental [38] and (with the 6-311G(2d,2p) basis set) calculated dipole moment curves of the FH molecule are presented. (For a previous investigation of the FH dipole moment curve, see ref. 39.)

The experimental dipole moment curve can be dissected into three parts. In the first section (0.6–1.2Å) μ(FH) increases linearly with increasing bond length R(FH). In the region between 1.2 and 1.6 Å, the dipole moment curve reaches a maximum (at 1.48 Å and μ=2.39 Debye) and turns over to decrease

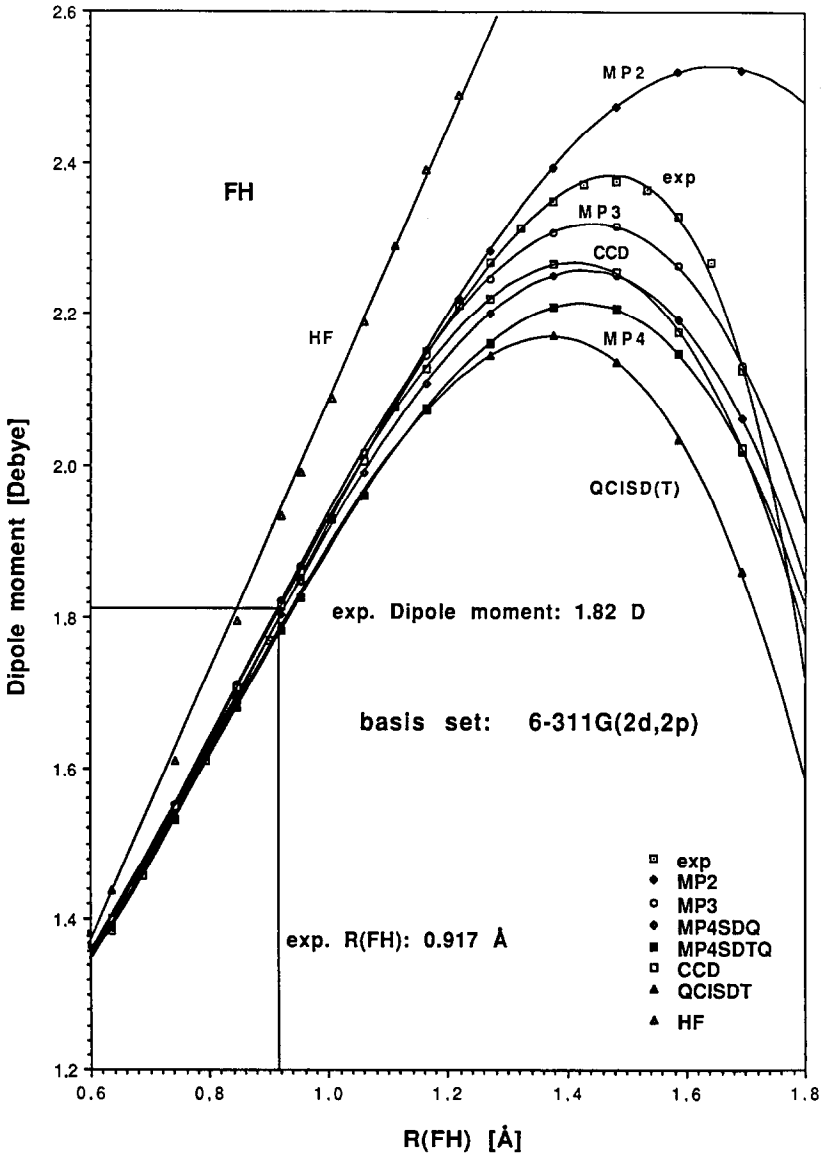

Fig. 12. Comparison of experimental [38] and calculated dipole moment curves of FH.

linearly with increasing R(FH) in the third section ($R > 1.6$ Å). The value of μ(FH) becomes zero for the case of the separated atoms.

All correlation corrected methods used in this work correctly describe the dipole moment curve of FH in the first section. Only the HF curve deviates from the experimental curve by predicting too large values of μ. Contrary to correlation-corrected methods, the HF description of the dipole moment curve

increases linearly in the whole range of calculated values without leading to a maximum. This, of course, has to do with the basic failure of HF to describe the dissociation of molecules correctly.

Of all the correlation-corrected ab initio methods used, MP3 and CCD give the best account of the experimental dipole moment curve (Fig. 12), which, of course, is due to a fortuitous cancellation of errors. In particular, MP3 predicts the position and the height of the maximum in the second section reasonably well. MP2, however, leads to a wrong description of the turning point of the dipole moment curve (see Fig. 12). MP4 and QCI lead to values of the FH dipole moment that are too small in the region between 1.2 and 1.8 Å (Fig. 12). Hence, the trends observed for calculated equilibrium dipole moments are conserved and amplified for larger R(FH). Clearly, the correct description of the dipole moment curve in the region of the turning point requires a correlation corrected method and a large basis set.

CALCULATION AND USE OF ACCURATE RESPONSE PROPERTIES

An accurate description of molecular multipole moments is highly desirable when investigating the interactions between molecules, in particular van der Waals complexes. The stability of such a complex is dominated by electrostatic interactions. As has been shown by Buckingham and Fowler [40], van der Waals complexes can be reasonably described by determining electrostatic interactions between the complex partners in terms of point multipoles that reflect the charge distribution in each monomer [41]. In this way the geometries and relative stabilities of a number of van der Waals complexes have been investigated at relatively low computational cost [40].

Since the interaction energy between two multipoles decreases with increasing distance R^m between the multipoles and since the power m of R increases with the order of the multipoles, monopole moments (atomic charges) and dipole moments dominate the electrostatic interactions between the molecular partners of a van der Waals complex. Hence, a reliable description of a van der Waals complex can only be expected if charges and dipole moments are correctly described. As is well known, a reliable description of a van der Waals complex requires at least a TZ basis set with two sets of polarization functions. We find that the same basis set quality is needed if molecular mono- and dipole moments have to be calculated.

Buckingham and Fowler noted that the multipole description of van der Waals complexes fails if the HF multipole moments of the complex partners are no longer accurate. The example they gave concerned complexes involving CO [40]. We want to add here other examples that underline the necessity of obtaining accurate response properties when calculating intermolecular complexes. These examples involve van der Waals complexes between ozone and H_2O [42], ethylene [43] or acetylene [44] as well as those between carbonyl

TABLE 4

Calculated atomic charges and dipole moments of ozone, O_3, and carbonyl oxide, CH_2OO, obtained with the 6-31G(d,p) basis set[a]

Molecule parameter	HF	MP2	MP4(SDTQ)	QCISD(T)	Exptl.
O_3					
$q(O_c)$	326	173	176	174	
$q(O_t)$	−163	−87	−88	−87	
μ	0.83	0.40	0.44	0.47	0.53
CH_2OO					
$q(CH_2)$	588	291	317	376	
$q(O_c)$	−195	34	−34	−65	
$q(O_t)$	−394	−325	−283	−311	
μ	5.46	3.44	3.25	3.76	

[a]Calculated at optimized geometries (see ref. 46). Charges, q, in melectron, dipole moments, μ, in Debye.

oxide, CH_2OO, and formaldehyde [45], which we have recently investigated in connection with a quantum chemical study of the ozonolysis reaction.

Calculated atomic charges and dipole moments of O_3 and CH_2OO are compared [46,47] in Table 4. The electronic structure of the two molecules is given in Scheme 2 in the form of a superposition of various resonance structures. The calculated data reveal that, at the HF level of theory, contributions of zwitter ionic structures (e.g. b in Scheme 2) to the molecular wave function are overestimated, thus leading to unreasonably large charges and dipole moments. As a consequence, electrostatic interactions between O_3 (CH_2OO) and another molecule within a van der Waals complex are exaggerated at the HF level. The stability of the van der Waals complex and the distance between the monomers in the complex are predicted to be too large at the HF level.

At the MP2 level, the contribution of the biradical structure a to the wave function is exaggerated, which is typical of MP2. As a consequence, atomic charges and the molecular dipole moment are calculated to be too small. Electrostatic interactions in a van der Waals complex containing either O_3 or CH_2OO are underestimated and therefore at MP2, the stability of the complex and the distance between the complex partners is too small. Thus MP2 leads to no improvement compared with the HF description of the van der Waals complexes.

At the MP4 and QCI level, more zwitter ionic structures are mixed into the wave function of either O_3 or CH_2OO, thus leading to reasonably accurate mono-

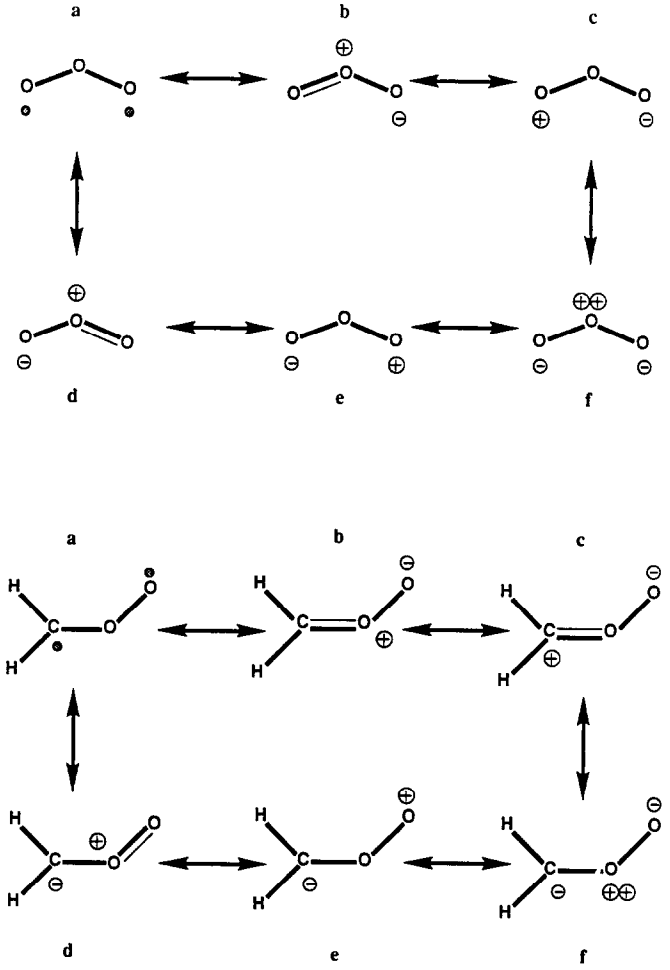

Scheme 2. Description of the electronic structure of ozone and carbonyl oxide in terms of resonance structures.

and dipole moments (see Table 4). Hence, a direct or a Buckingham–Fowler description of van der Waals complexes involving these molecules can only be successful if MP4 or QCI is applied [42–45]. It is wrong, in such a case, to hope that known deficiencies in the ab initio description of the complex partners cancel out if the complex itself is calculated.

SUMMARY

(1) Response properties (electron density distributions, atomic charges, dipole moments, and quadrupole moments) of 20 small molecules have been

calculated by nine different ab initio methods utilizing analytical energy derivatives derived earlier [17,18,20,21].

(2) A detailed analysis of the calculated values of the response properties of CO suggests an oscillation of correlation corrections of these properties that persists to the fifth order perturbation theory and probably also to the sixth order. Convergence of dynamical correlation corrections to molecular properties calculated at the MPn level of theory for molecules in their equilibrium geometry is much slower than one generally tends to believe. In a critical case such as the CO molecule, MP4 is not sufficient to obtain accurate response properties, in particular accurate atomic charges and an accurate dipole moment. QCI and CC methods that contain important MP5 and higher-order contributions lead to better values.

(3) If sufficiently large basis sets are used (DZP or larger), then oscillations of correlation corrections are almost independent of the basis set. This can be exploited to select method and basis set in a way that leads to a cancellation of basis set and correlation errors and hence to reasonably accurate response properties.

(4) Correlation corrections to the lower multipole moments are important when the molecule in question possesses multiple bonds, in particular semipolar bonds. In these cases, MP4 or QCI calculations are needed to get reasonably accurate multipole moments. In all other cases, basis set effects are more important than correlation corrections. Hence, it is sufficient to carry out MP2 calculations with a TZ+2P basis set to get reasonably accurate values.

(5) Correlation corrections to molecular response properties become large if they are calculated for interatomic distances far from the equilibrium value. For example, reliable dipole moment curves can only be obtained when using elaborate correlation corrected methods. However, computational costs can be cut down by using a method that provides reasonable equilibrium properties due to cancellation of errors.

(6) The accurate description of molecular complexes that are dominated by electrostatic interactions depends on the accurate description of the response moments of the complex partners. Hence, the same level of theory that is needed to describe atomic charges and dipole moments of 1,3-dipolar molecules such as ozone or carbonyl oxide is also needed to describe van der Waals complexes involving these molecules.

ACKNOWLEDGEMENTS

This work was supported by the Swedish National Science Foundation (NFR). All calculations have been carried out at the Nationalet Superdator Centrum (NSC) at the University of Linköping. DC and EK thank the NSC for a generous allotment of computer time.

REFERENCES

1 C. Møller and M.S. Plesset, Phys. Rev., 46 (1934) 618.
2 J.A. Pople, J.S. Binkley and R. Seeger, Int. J. Quantum Chem. Symp., 10 (1976) 1.
3 R. Krishnan and J.A. Pople, Int. J. Quantum Chem., 14 (1978) 91.
4 (a) R. Krishnan, M.J. Frisch and J.A. Pople, J. Chem. Phys., 72 (1980) 4244.
(b) M.J. Frisch, R. Krishnan and J.A. Pople, Chem. Phys. Lett., 75 (1980) 66.
5 (a) R.J. Bartlett and I. Shavitt, Chem. Phys. Lett., 50 (1977) 190.
(b) R.J. Bartlett and G.D. Purvis, J. Chem. Phys., 68 (1978) 2114.
(c) R.J. Bartlett, H. Sekino and G.D. Purvis, Chem. Phys. Lett., 98 (1983) 66.
6 S.R. Langhoff and E.R. Davidson, Int. J. Quantum Chem. Symp., 10 (1976) 1.
7 W. Meyer, Int. J. Quantum Chem., 5 (1971) 341; J. Chem. Phys., 58 (1973) 1017.
8 R. Ahlrichs, P. Scharf and C. Ehrhardt, J. Chem. Phys., 82 (1985) 890.
9 J.A. Pople, M. Head-Gordon and K. Raghavachari, J. Chem. Phys., 87 (1987) 5968.
10 K. Raghavachari, J.A. Pople, E.S. Replogle and M. Head-Gordon, J. Phys. Chem., 94 (1990) 5579.
11 R.D. Amos, Chem. Phys. Lett., 88 (1982) 89.
12 (a) E.A. Salter, G.W. Trucks, G. Fitzgerald and R.J. Bartlett, Chem. Phys. Lett., 141 (1987) 61.
(b) G.W. Trucks, E.A. Salter, C. Sosa and R.J. Bartlett, Chem. Phys. Lett., 147 (1988) 359.
13 G.W. Trucks, E.A. Salter, J. Noga and R.J. Bartlett, Chem. Phys. Lett., 150 (1988) 37.
14 (a) R. McWeeny, Rev. Mod. Phys., 32 (1960) 335; Phys. Rev., 126 (1962) 1028.
(b) R.M. Stevens, R.M. Pitzer and W.N. Lipscomb, J. Chem. Phys., 38 (1963) 550.
(c) J. Gerratt and I.M. Mills, J. Chem. Phys., 49 (1968) 1719.
15 C. Sosa, W.G. Trucks, G.D. Purvis III and R.J. Bartlett, J. Mol. Graphics, 7 (1989) 28.
16 J.A. Pople, R. Krishnan, H.B. Schlegel and J.S. Binkley, Int. J. Quantum Chem. Symp., 13 (1979) 225.
17 J. Gauss and D. Cremer, Chem. Phys. Lett., 138 (1987) 131.
18 J. Gauss and D. Cremer, Chem. Phys. Lett., 153 (1988) 303.
19 N.C. Handy, R.D. Amos, J.F. Gaw, J.E. Rice and E.D. Simandiras, Chem. Phys. Lett., 120 (1985) 151.
20 N.C. Handy and H.F. Schaefer III, J. Chem. Phys., 81 (1984) 5031.
21 (a) J. Gauss and D. Cremer, Chem. Phys. Lett., 150 (1988) 280.
(b) J. Gauss and D. Cremer, Chem. Phys. Lett., 163 (1989) 549.
22 J. Gauss and D. Cremer, Adv. Quantum Chem., in press.
23 R.S. Mulliken, J. Chem. Phys., 23 (1955) 1833, 1841, 2338, 2343.
24 (a) R.F.W. Bader and T.T. Nguyen-Dang, Adv. Quantum Chem., 14 (1981) 63.
(b) R.F.W. Bader, T.S. Slee, D. Cremer and E. Kraka, J. Am. Chem. Soc., 105 (1983) 5061.
25 (a) J.A. Pople, R. Krishnan, H.B. Schlegel and J.S. Binkley, Int. J. Quantum Chem., 14 (1978) 545.
(b) R.J. Bartlett and G.D. Purvis, Int. J. Quantum Chem., 14 (1978) 561.
26 J. Gauss, E. Kraka, F. Reichel and D. Cremer, COLOGNE, University of Göteborg, 1990.
27 P.C. Hariharan and J.A. Pople, Theor. Chim. Acta, 28 (1973) 213.
28 (a) First row: R. Krishnan, J.S. Binkley, R. Seeger and J.A. Pople, J. Chem. Phys., 72 (1980) 650.
(b) Second row: A.D. McLean and G.S. Chandler, J. Chem. Phys., 72 (1980) 5639.
29 (a) A.K. Siu and E.R. Davidson, Int. J. Quantum Chem., 4 (1970) 233.
(b) S. Green, Chem. Phys., 54 (1971) 827.
(c) F.P. Billingsley II and M. Krauss, J. Chem. Phys., 60 (1974) 4130.
(d) K. Kirby-Docken and B. Liu, J. Chem. Phys., 66 (1977) 4309.
(e) P.G. Jasien and C.E. Dykstra, Int. J. Quantum Chem., 28 (1985) 411.
(f) R. Jaquet, W. Kutzelnigg and V. Staemmler, Theor. Chim. Acta, 54 (1980) 205.

30 (a) R. Krishnan and J.A. Pople, Int. J. Quantum Chem., 20 (1981) 1067;
(b) A.J. Sadlej, Theor. Chim. Acta, 47 (1978) 205.
31 (a) G.E. Scuseria and H.F. Schaefer III, Chem. Phys. Lett., 148 (1988) 205.
(b) J. Watts, G.W. Trucks and R.J. Bartlett, Chem. Phys. Lett., 157 (1989) 359.
32 S. Green, Adv. Chem. Phys., 25 (1974) 179.
33 (a) R.D. Nelson, D.R. Lide and A.A. Maryott, NSRDA-NBS 10, U.S. Government Printing Office, Washington DC, 1967.
(b) A.L. McClellan, Tables of Experimental Dipole Moments, Vol. 2, W.H. Freeman, San Francisco, 1963, Rahara Enterprises, El Ceritos, California, 1974.
34 (a) P.M.W. Gill and L. Radom, Chem. Phys. Lett., 132 (1986) 16.
(b) N.C. Handy, P.J. Knowles and K. Somasundram, Theor. Chim. Acta, 68 (1985) 87.
(c) P.J. Knowles, K. Somasundram and N.C. Handy, Chem. Phys. Lett., 113 (1985) 8.
35 (a) S.A. Kucharski, J. Noga and R.J. Bartlett, J. Chem. Phys., 90 (1989) 7282.
(b) W.D. Laidig, G. Fitzgerald and R.J. Bartlett, Chem. Phys. Lett., 113 (1985) 151.
(c) see ref. 10.
36 Zhi He and D. Cremer, Int. J. Quantum Chem. Symp., in press.
37 W.J. Hehre, L. Radom, P. v. R. Schleyer and J.A. Pople, Ab Initio Molecular Orbital Theory, Wiley, New York, 1986.
38 R.N. Sileo and T.A. Cool, J. Chem. Phys., 65 (1976) 117.
39 P.G. Jasien and C.E. Dykstra, Int. J. Quantum Chem. Symp., 17 (1983) 289.
40 A.D. Buckingham and P.W. Fowler, Can. J. Chem., 63 (1985) 2018.
41 A. Stone, J. Chem. Phys. Lett., 83 (1981) 233.
42 J.Z. Gillies, C.W. Gillies, R.D. Suenram, F.J. Lovas, T. Schmidt and D. Cremer, J. Mol. Spectrosc., 146 (1991) 493.
43 J.Z. Gillies, C.W. Gillies, R.D. Suenram, F.J. Lovas, E. Kraka and D. Cremer, J. Am. Chem. Soc., 113 (1991) 2412.
44 J.Z. Gillies, C.W. Gillies, R.D. Suenram, K. Matsumura, F.J. Lovas, E. Kraka and D. Cremer, J. Am. Chem. Soc., in press.
45 D. Cremer, M. McKee and T.P. Radakrishnan, in preparation.
46 E. Kraka, F. Reichel and D. Cremer, in preparation.
47 J.F. Stanton, W.N. Lipscomb, D.H. Magers and R.J. Bartlett, J. Chem. Phys., 90 (1989) 1077.